The EMBO Journal vol.15 no.23 pp.6495–6505, 1996

Preformed cytoplasmic nucleocapsids are not necessary for alphavirus budding

Kerstin Forsell, Gareth Griffiths[1] and Henrik Garoff[2]

Department of Bioscience at Novum, S-141 57 Huddinge, Sweden and [1]European Molecular Biology Laboratory, Postfach 10.2209, 69012 Heidelberg, Germany

[2]Corresponding author

According to the present model for assembly of alphaviruses, e.g. Semliki Forest virus (SFV), the viral genome is first encapsidated into a nucleocapsid (NC) in cytoplasm and this is then used for budding at plasma membrane (PM). The preformed NC is thought to act as a template on which the viral envelope can be organized. In the present work we have characterized two SFV deletion mutants which did not assemble NCs in the cytoplasm but which instead appeared to form NCs at the PM simultaneously with virus budding. The deletions were introduced in a conserved 14 residue long linker peptide that joins the amino-terminal RNA-binding domain with the carboxy-terminal serine-protease domain of the capsid protein. Despite the deletions and the change in morphogenesis, wild-type (wt)-like particles were produced with almost wt efficiency. It is suggested that the NC assembly defect of the mutants is rescued through spike–capsid interactions at PM. The results show that the preassembly of NCs in the cytoplasm is not a prerequisite for alphavirus budding. The apparent similarities of the morphogenesis pathways of wt and mutant SFV with those of type D and type C retroviruses are discussed.

Keywords: alphavirus/budding/C- and D-type retrovirus/nucleocapsid

Introduction

The assembly of alphaviruses such as Semliki Forest virus (SFV), Sindbis virus (SIN) and Ross River virus (RRV) is today better characterized than that of any other enveloped animal virus (Strauss and Strauss, 1994). According to the present model, alphavirus assembly involves two parallel processes, that of spike assembly in the context of cellular membranes and nucleocapsid (NC) assembly in the cell cytoplasm. Spike complexes and NCs are routed separately to the plasma membrane (PM) where final virus maturation occurs by budding.

The viral structural proteins that direct the assembly processes are the capsid protein C and the two membrane proteins p62 and E1. These are translated sequentially in the order C-p62-E1 from a common coding unit in the viral subgenome, the 26S RNA molecule. The C protein consists of two distinct domains, a carboxy-terminal one which functions as a protease to release the C protein from the nascent polyprotein chain and an amino-terminal one that recognizes and encapsidates the viral genome, a 42S RNA molecule (Weiss *et al.*, 1989; Choi *et al.*, 1991; Geigenmüller-Gnirke *et al.*, 1993; Forsell *et al.*, 1995). The C protein does not bind the genome directly after synthesis but it associates first with ribosomes which mediate their transfer to the 42S RNA genome (Söderlund and Ulmanen, 1977). The formation of a new NC (sedimentation value = 140S) occurs very rapidly and appears to involve one intermediate structure which consists of a 42S RNA molecule complexed to a subset of C molecules (sedimentation value = 90S) (Ulmanen *et al.*, 1976; Ulmanen, 1978).

The spike assembly is initiated by the synthesis and insertion of the p62 and E1 chains into the membrane of the endoplasmic reticulum (ER). The two membrane proteins heterodimerize into strong p62–E1 complexes, which upon transport to PM become converted into labile E2–E1 complexes by cleavage of the p62 subunit (Wahlberg *et al.*, 1989). The budding reaction at the PM is driven by the binding of the spikes to the NC surface and probably also by spike–spike interactions in the plane of the membrane (Suomalainen *et al.*, 1992; Cheng *et al.*, 1995). Altogether, the assembly process results in the formation of an enveloped particle with one 42S RNA and 240 copies of C, E2 and E1 (Laine *et al.*, 1973; Vogel *et al.*, 1986; Paredes *et al.*, 1993; Cheng *et al.*, 1995; Fuller *et al.*, 1995). Both the NC and the envelope are organized according to T = 4 symmetry. However, in the case of the NC the C molecules are associated in pentameric and hexameric capsomers, whereas the membrane proteins form 80 spikes each consisting of three copies of a heterodimer.

A central part of the alphavirus assembly model described above is the presence of a cytoplasmic pool of NCs that is used for virus production (Strauss and Strauss, 1994). These preassembled NCs are thought to serve as templates around which the viral membrane can be organized. In this work we describe SFV variants, created by *in vitro* mutagenesis of the SFV cDNA clone, which have lost the capacity to form cytoplasmic NC structures but which are still budding competent. The SFV mutations were directed to a gene region encoding a stretch of conserved amino acids in the junction between the RNA-binding and protease domains of the C protein. These results show that a cytoplasmic pool of preassembled NCs is not necessary for alphavirus budding and release.

Results

Construction and expression of SFV mutants

The RNA-binding domain of the SFV C protein is characterized by several clusters of basic residues and extends from the amino-terminus to Lys104 (Figure 1). The serine-

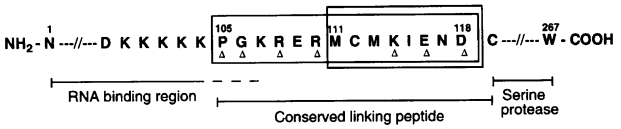

Fig. 1. Amino acid sequence of conserved linking peptide. The amino acid sequence of the junction region between the amino-terminal RNA-binding and the carboxy-terminal protease domain of SFV C protein is shown using the one-letter code for amino acid residues. Numbers indicate order of residue in sequence. Triangles indicate residues which are conserved in C proteins of different alphaviruses. Deleted regions are boxed.

protease domain starts with Cys119 and extends to the carboxy-terminal Trp267. In between the two functional domains there is a peptide with a sequence of amino acid residues which is very conserved in different alphaviruses (Garoff *et al.*, 1980; Rice and Strauss, 1981; Dalgarno *et al.*, 1983; Kinney *et al.*, 1986; Chang and Trent, 1987; Hahn *et al.*, 1988; Levinson *et al.*, 1990; Strauss and Strauss, 1994; Rümenapf and Strauss, 1995). In order to investigate its role in virus replication we created two deletion variants of the SFV genome: SFV-CΔ105–118 which lacks the complete region encoding the conserved amino acid sequence and SFV-CΔ111–118 which lacks only the distal half of this region (Figure 1). Deletions were performed in pSP6–SFV4, which contains the complete DNA copy of the SFV genome (Liljeström *et al.*, 1991). For expression analysis, replication-competent RNA was transcribed from corresponding plasmids *in vitro* and used for transfection of BHK 21 cells by electroporation.

We first followed the general features of viral protein synthesis and particle assembly in the transfected cells by a pulse–chase experiment using [^{35}S]methionine. SDS–gel analysis of viral proteins from cells chased for 15 min shows that both deletion variants directed synthesis of C, p62 and E1 proteins at levels similar to wild-type (wt) (Figure 2A, lanes 1, 6 and 11). After a 3 h chase the majority of p62 proteins was processed into E2 which, when reduced, co-migrates with E1 (Figure 2A, lanes 2, 7 and 12). Analysis of pelleted material from the media of the mutant RNA-transfected cells that had been chased for 3 h showed that virus-like particles containing all structural proteins had been released (Figure 2A, lanes 9 and 14). The amounts of the released mutant particles appeared to be similar to that of wt (Figure 2A, lane 4). In a close-by comparison (Figure 2B) it is evident that the mutant C proteins migrated slightly more quickly than wt C protein. This corresponds to the deletions introduced. The media were also screened for infectious virus by plaque assay. The results indicated that infectious particles were produced from both SFV-CΔ105–118 and SFV-CΔ111–118 RNA-transfected cells. Thus, the mutant viruses were replication competent despite the C protein deletion. This facilitated the preparation of mutant virus stocks and the use of infection, in addition to RNA transfection, as a way to introduce the mutant genomes into cells for further phenotype analyses. In order to avoid the possible generation and amplification of suppressor mutants in stock preparations we used the media of transfected cells (titre ≈10^8 p.f.u./ml) directly, without further passaging.

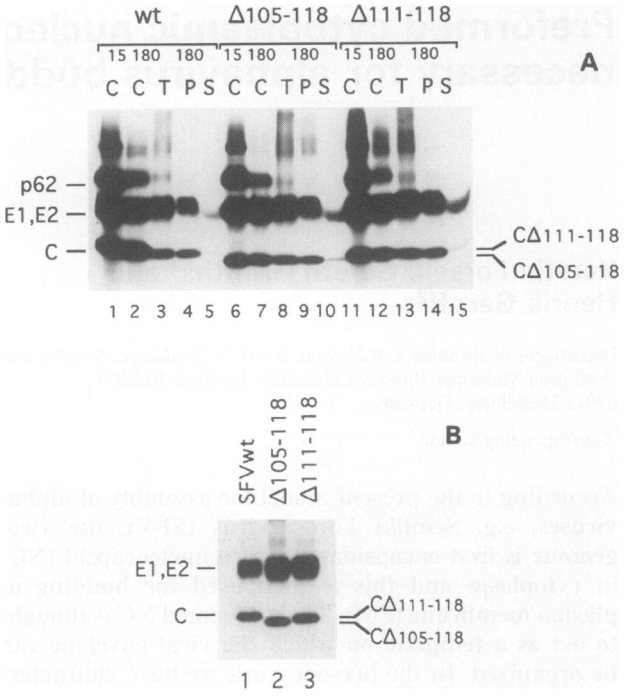

Fig. 2. Viral protein synthesis and assembly in cells transfected with wt and mutant RNA. Cells were transfected with RNA, pulse-labelled, chased and lysed as described in text. Samples of cell lysates (C) and media pellets (P) were analysed by SDS–PAGE together with TCA precipitates of media supernatants (S) and unfractionated (total, T) media. Corresponding amounts of cell lysate and media samples were analysed. (**A**) Analyses of wt, SFV-CΔ105–118 and SFV-CΔ111–118 RNA-transfected cells. (**B**) Close-by analysis of virus pellets.

Efficiency of virus release

Cells were transfected with equal amounts of wt or mutant RNA. Pairs of cultures from each transfection were prepared and labelled with [^{35}S]methionine for 15 min. One of them was chased for 5 min and then lysed. This sample was used to determine the total amount of radioactive viral protein that was synthesized during the pulse. The other culture was used for the measurement of released virus. Therefore, the medium was replaced every hour and virus particles were pelleted from each medium sample. Cell lysates and virus pellets were analysed by SDS–PAGE and radioactivities in the viral membrane protein bands quantified. The values were used for the calculation of released virus, which is expressed as membrane protein in virions as a percentage of initially synthesized membrane protein; the results are shown in Figure 3. In the case of the wt, ~8% of the membrane proteins was released as part of virus particles in 5 h. This efficiency of virus release is very similar to that reported previously for Sindbis virus (Scheele and Pfefferkorn, 1969). The efficiency of release of SFV-CΔ111–118 was found to be only slightly lower than that of wt, whereas SFV-CΔ105–118 was somewhat more inhibited; ~7% and 5% respectively of labelled spikes were released as part of particles in 5 h. We conclude that the mutants are able to drive particle assembly almost as efficiently as wt, despite the deletion in the C protein.

Characteristics of mutant virus particles

Wild-type and mutant virus particles which were labelled with [^{35}S]methionine in their structural proteins and with

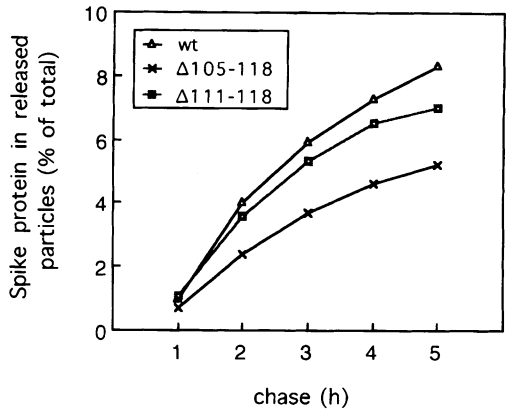

Fig. 3. Efficiency of virus release. Cell cultures were transfected with wt and mutant RNAs, labelled, chased and lysed as described in text. Virus particles were isolated by pelletization from the media samples. Samples of lysates and media pellets were analysed by SDS–PAGE and radioactive viral membrane proteins were quantified. The graph shows the fraction (%) of the pulse-labelled membrane (spike) proteins which is released into media with time.

[^{3}H]uridine in their RNA were used for sedimentation in sucrose gradients (Figure 4). The results show that both mutants sedimented to the same position in the gradient as did wt. This suggests that mutant and wt virus particles are similar in size. We also calculated the protein:RNA ratio using the [^{35}S]methionine and [^{3}H]uridine radioactivities in peak fractions. As shown in Table I, this ratio is very similar for mutant and wt virus, suggesting that RNA incorporation into mutant virus was unaffected.

To determine the protein stoichiometry in the particles we isolated virions from media of cells that had been labelled with [^{35}S]methionine for 6 h. These preparations were analysed by SDS–PAGE and the radioactivities in C, E2 and E1 protein bands were measured. The values were corrected for the methionine content in the respective protein and used for calculation of the ratio of membrane protein (E1 + E2) to C protein. This was found to be close to 1:1 for mutant as well as for control virus, suggesting that both of the mutants contain a wt-like protein composition in their NC and membrane (Table I). Electron microscopic (EM) analyses of infected cells, which will be described later, showed furthermore that the released mutant particles have a wt-like appearance. However, when the mutant virus particles were treated with NP-40, which solubilized the membrane around the NCs, the latter did not persist as 150S subviral structures, as is the case with wt (Kääriäinen and Söderlund, 1971), but aggregated into larger complexes. The corresponding sedimentation analyses are shown in Figure 5. The upper panel shows RNA and protein profiles in gradients where released NCs of double-labelled wt SFV and SFV-CΔ111–118 have been sedimenting. Note the absence of the 150S NC peak in the middle of the gradient where the mutant has been analysed. Instead, RNA and protein accumulate in the pellet. The lower panel shows SDS–gel analyses of viral proteins in fractions and pellets of gradients where solubilized ^{35}S-labelled wt SFV, SFV-CΔ105–118 and SFV-CΔ111–118 have been run. Note the almost complete pelletization of the C protein of the mutant viruses. This is in clear contrast to wt SFV where most of the C protein is migrating as 150S NCs in the gradient. Thus, these

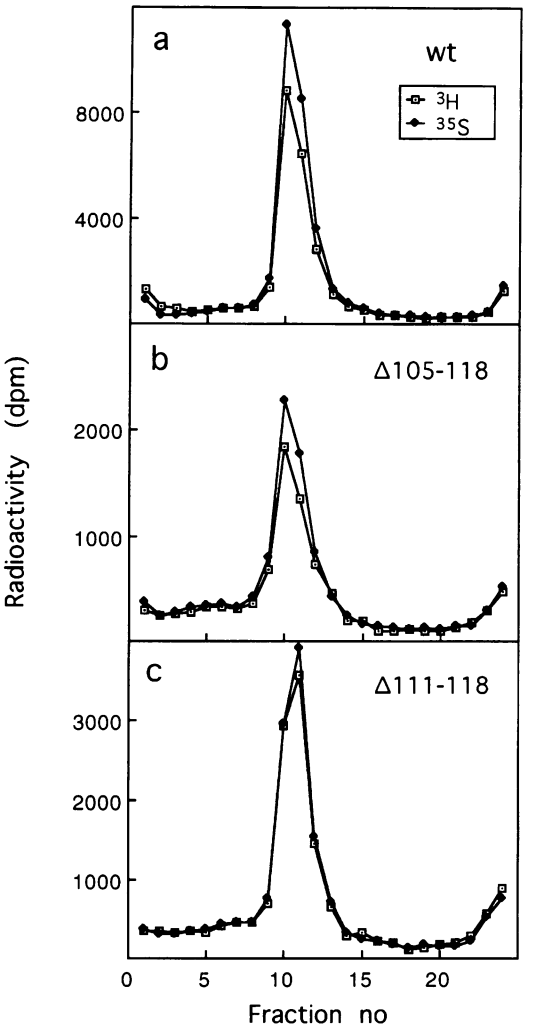

Fig. 4. Velocity sedimentation analyses of wt and mutant virus particles. Double-labelled virus particles were run on 15–30% (w/w) sucrose gradients, fractionated and analysed for radioactivity by liquid scintillation counting as described in text. Figure shows analysis of (**a**) wt, (**b**) SFV-CΔ105–118, and (**c**) SFV-CΔ111–118. The top of each gradient is to the right.

Table I. Composition of virus particles

Virus	RNA/protein[a]		
	I	II	E1 + E2/C[b]
SFV wt	0.77	1.5	1.09
Δ105–118	0.81	1.7	1.14
Δ111–118	0.91		1.08

[a]Ratio is calculated by dividing [^{3}H]uridine radioactivity of virus peak in analysis shown in Figure 4 by that of [^{35}S]methionine. Results from two separate experiments are given. The difference between the values of the two experiments is due to variation in incorporation of label.
[b]The ratio of membrane to C protein was calculated using [^{35}S]methionine-labelled virus preparations as described in text. Values represent mean of three experiments.

results suggest that the mutant NCs are unstable without a surrounding membrane.

We also measured the specific activity of the mutant virus. For this purpose, cells were transfected and pulse-labelled for 6 h with [^{35}S]methionine. The amount of

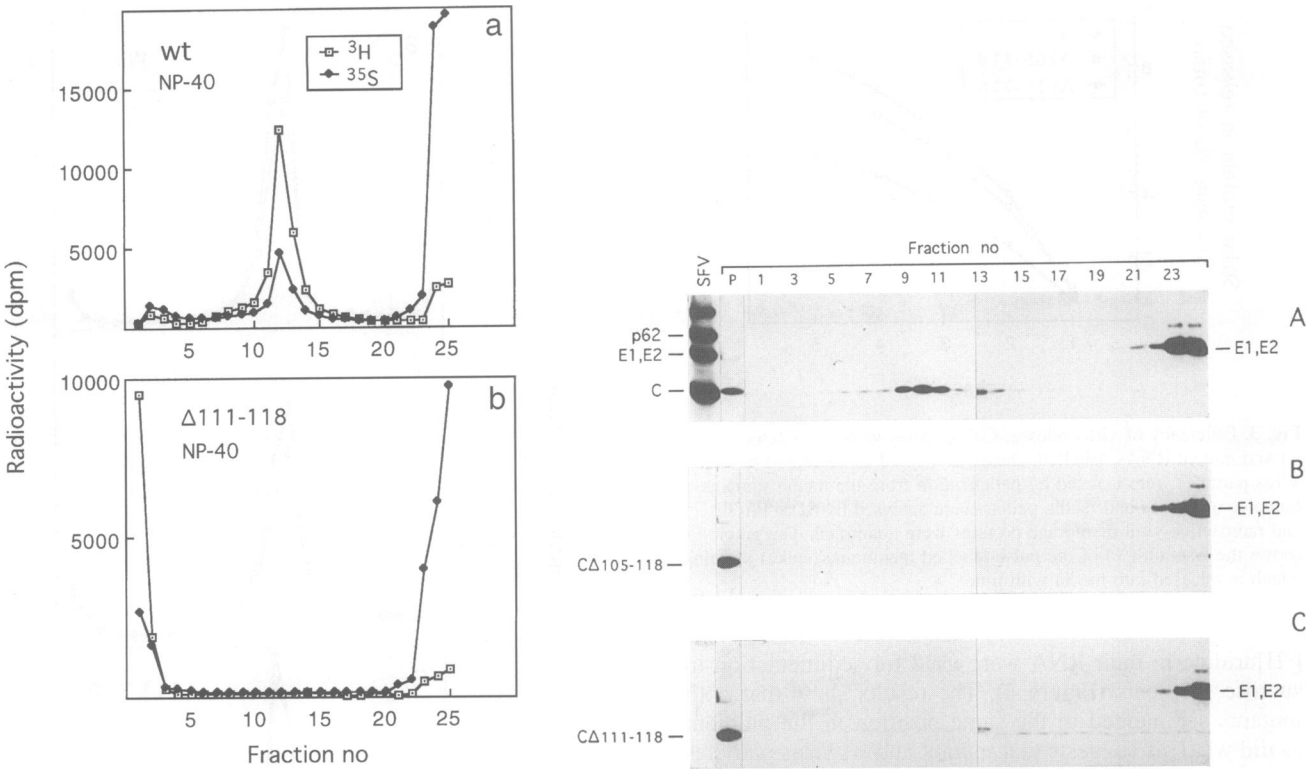

Fig. 5. Velocity sedimentation analyses of NCs of wt and mutant virus particles. Double-labelled ^{35}S and ^{3}H and single-labelled ^{35}S preparations of wt and mutant virus particles were incubated in NP-40-containing buffer to solubilize the envelope and release the NC. The samples were then run on 15–30% (w/w) sucrose gradients containing NP-40. Left panel: radioactivity profiles of the viral RNA and protein in gradients where (**a**) solubilized wt SFV and (**b**) SFV-CΔ111–118 have been run, respectively. Right panel: SDS gel analyses of ^{35}S-labelled viral proteins in fractions of gradients where (**A**) solubilized wt SFV, (**B**) SFV-CΔ105–118 and (**C**) SFV-CΔ111–118 have been subjected to sedimentation.

radioactive particles in media and their plaque-forming capacity were measured. The specific infectivities (plaques per radioactive virus) were calculated and expressed relative to wt. The result showed that the mutant particles had reduced specific infectivities. These were 12% (SFV-CΔ105–118) and 16% (SFV-CΔ111–118) of the wt value. The values represent the mean of three determinations.

The mutant virus does not assemble NCs in cytoplasm

Intracellular alphavirus NCs can easily be detected by sedimentation analysis of cell lysates or homogenates. In contrast, the NC intermediate structures and the ribosome–C protein complexes are more difficult to identify by such analyses, partly because of their more transient nature in the assembly process and partly because they appear in the form of large and heterogeneous polysomes in the cytoplasm (Söderlund and Ulmanen, 1977; Ulmanen, 1978). The latter problem can be overcome by treating the lysate with EDTA, which dissociates the polysomes. In order to follow the NC assembly of the mutants by sedimentation analysis we performed two types of labelling experiments of transfected cells. In one we labelled the viral proteins with [^{35}S]methionine and followed the C protein distribution; in the other we labelled the RNA with [^{3}H]uridine, in addition, in order to co-monitor viral protein and RNA.

Figure 6a and b show sedimentation analyses of a lysate from wt RNA-transfected cells. In Figure 6a, the lysate had been treated with $MgCl_2$ to preserve the polysomes and in Figure 6b with EDTA to dissociate the same. In both analyses the solubilized spike proteins (p62, E2 and E1) remain in the top fractions (1–3) whereas the majority of the C protein is seen as a clear peak (band) in the middle of the gradient. This corresponds to 150S intracellular NCs (Söderlund, 1973). Some C protein is also seen in the pellet fraction, especially in the analysis of the $MgCl_2$-treated sample. Part of the latter material can be dissociated with EDTA into smaller complexes which appear to locate in fractions 4–7 (Figure 6b).

The corresponding analyses of a lysate prepared from SFV-CΔ105–118 RNA-transfected cells are shown in Figure 6c and d. The most striking finding is the absence of a 150S NC peak in these gradients. The analysis of the $MgCl_2$-treated lysate (Figure 6c) shows that the majority of the C protein is now present in the pellet and the remainder is distributed in the upper region of the gradient. After EDTA treatment the pelletizable structures dissociate into much smaller C-complexes. In several repeated experiments this material located ultimately in two partially overlapping peaks (fractions 4–5 and 7–8). Identical results were obtained with the other mutant (data not shown).

All of our RNA labelling experiments with [^{3}H]uridine were performed in the presence of 1 μg/ml actinomycin D. This inhibits host RNA synthesis and allows the specific labelling of viral 42S and 26S RNAs. The effect of actinomycin D treatment on host RNA synthesis was studied by labelling non-transfected cells with [^{3}H]uridine in the presence or absence of actinomycin D and per-

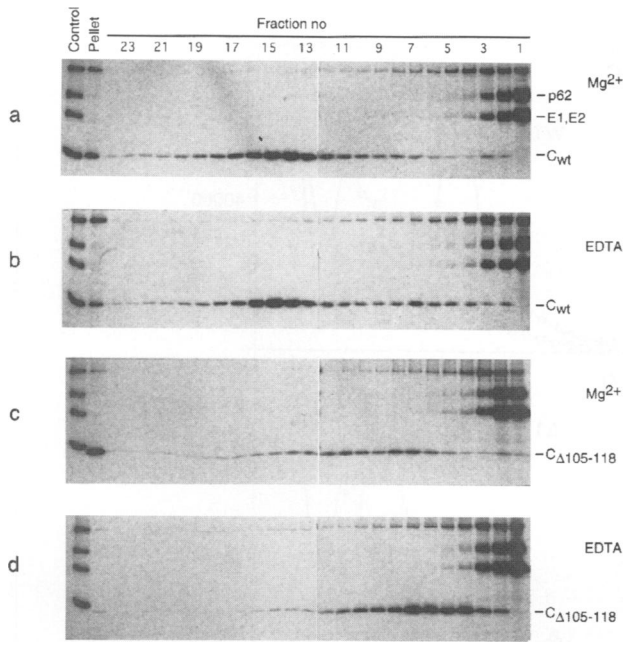

Fig. 6. Analysis by SDS–PAGE of sedimented C protein complexes from lysates of transfected cells. Cells were transfected with wt or mutant RNA, pulse-labelled for 30 min with [^{35}S]methionine and chased for 15 min. Cells were lysed in an NP-40-containing buffer, mixed with $MgCl_2$ or EDTA and samples run on 15–30% (w/w) sucrose gradients. Viral proteins in gradient fractions were analysed by SDS–PAGE. The top of each gradient is to the right. The lane marked 'Control' represents an analysis of a lysate from cells that have been infected and labelled with wt SFV. The upper band seen in analyses of top fractions represents untranslocated and uncleaved p62–E1 polyprotein.

forming sedimentation analyses of corresponding lysates. The results are shown in Figure 7a and b: without the inhibitor, large-sized [^{3}H]uridine-labelled material, most likely representing ribosome subunits, is seen to enter into fractions 4–6 of the gradient. However, in the presence of the inhibitor this material is completely unlabelled.

Figure 7c shows ^{3}H and ^{35}S profiles of a sedimentation analysis of an EDTA-treated lysate from wt RNA-transfected and double-labelled cells. Because actinomycin D was present during the labelling, all ^{3}H label represents viral RNA except in top fractions 1 and 2, which contain some free [^{3}H]uridine. Furthermore, from the analysis shown in Figure 6b, we can deduce that practically all ^{35}S radioactivity below fractions 3–4 in Figure 7c must represent labelled C protein. The radioactivity profiles of the latter sedimentation show a major ^{35}S- and ^{3}H-labelled band in the middle of the gradient. This represents encapsidated viral genomes, i.e. NCs. In addition, there is a broad peak of labelled viral RNA in fractions 5–8. In this region one can distinguish a peak in fraction 5 and a peak-shoulder near fraction 8. The material in fractions 8 and 5 probably corresponds to the NC intermediate complexes and the 26S RNA–host protein complexes that have been found and characterized previously in wt SFV-infected cells (Ulmanen *et al.*, 1976).

Figure 7d and e show corresponding analyses of mutant RNA-transfected cells. In neither analysis is there any indication of 150S NCs being present. Instead, these sedimentation analyses show a very prominent viral RNA peak in fraction 8 and a smaller one in fraction 5. The migration of these RNA complexes correspond to the NC intermediate and the 26S RNA–host protein complexes of wt (Figure 7c). The protein profiles of the sedimentation analyses in Figure 7d and e indicate accumulation of viral proteins in the top half of the gradients. There is a partially resolved peak in fraction 8 and a second peak or shoulder in fraction 6. This probably corresponds to C protein that is part of NC intermediate structures and ribosome–C protein complexes, respectively. The protein label at the top represents predominantly soluble spike proteins. Note the much lower C protein:RNA ratio in the NC intermediates (fraction 8 in Figure 7d and e) than in the completely assembled NCs (fraction 12 in Figure 7c). This is consistent with the intermediate nature of these complexes, i.e. they consist of a viral genome which is not fully encapsidated with C protein. Taken together, the results of these analyses suggest that the mutant viruses are not able to complete the NC assembly process in cell cytoplasm, but instead accumulate NC intermediate structures and ribosome–C protein complexes.

A trivial explanation to the absence of NCs in the NP-40 lysates of mutant RNA-transfected cells is that mutant NCs are sensitive to NP-40 due to the deletion introduced into the C polypeptide. In order to test for this possibility we used EDTA-treated homogenates from transfected and [^{35}S]methionine-labelled cells instead of NP-40 lysates for our sedimentation analyses. However, the results did not change: most mutant C proteins migrated as a double band in fractions 7–8 and 5, and almost none of it was observed in the region of wt NCs. This is shown in Figure 8 (lower panel), for SFV-CΔ105–118. The figure represents a quantitation of C and spike proteins in gradient fractions. Note that both in the case of the mutant and wt, a significant amount of C protein sediments with membranes. This corresponds most likely to C protein which is involved in virus budding at the cell surface.

The results of the sedimentation analyses were confirmed by EM analyses of cells infected with mutant or wt SFV. In the latter case the analyses showed typical 35 nm NCs which were scattered around in the cytoplasm as separate particles or groups of particles (Figure 9A). A similar analysis of the SFV-CΔ105–118 RNA-transfected cells showed the total absence of NC particles in cytoplasm (Figure 9B). This was also true for the SFV-CΔ111–118 RNA-transfected cells (not shown).

Intracellular C protein complexes and virus release

In order to study the utilization of the cytoplasmic C protein complexes for mutant virus formation we pulse-labelled transfected cells with [^{35}S]methionine (15 min) and followed the pool sizes of cell-associated and viral C protein with time (1, 3 and 5 h). Wt was studied as control. Cells were lysed in an NP-40-containing buffer and fractionated into a supernatant and a low-speed pellet. The virus in the media was isolated by pelletization. All samples were analysed by SDS–PAGE and the C protein quantified. According to our earlier results (Figures 6 and 7), the analysis of the lysate supernatants of the wt sample should give the approximate pool size of C protein in NCs and that of mutant samples should give the amount of C protein in NC intermediates and ribosome–C protein complexes, respectively. The C protein in the lysate pellet represents a pool of NP-40-non-extractable C protein and

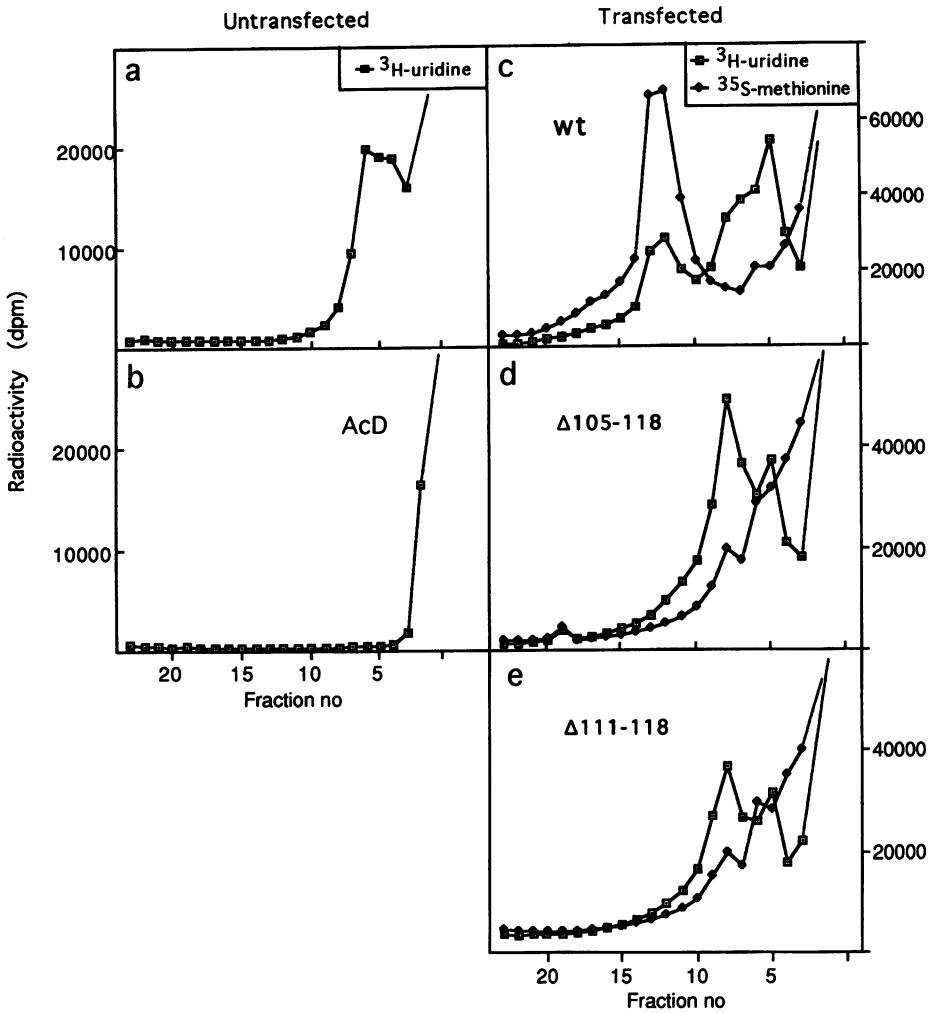

Fig. 7. Sedimentation analyses of viral RNA and protein complexes in lysates of transfected cells. Transfected cells were double-labelled with [^{3}H]uridine for 3.5 h and [^{35}S]methionine for 15 min in the presence of actinomycin D (**c–e**). Untransfected cells were labelled only with [^{3}H]uridine in the presence (**b**) or absence (**a**) of actinomycin D. Lysates were prepared and analysed by sedimentation in a 15–30% (w/w) sucrose gradient. Each fraction was then analysed for ^{3}H and ^{35}S radioactivity using liquid scintillation counting. Note that the values for fractions 1 of gradients (a) and (b) and fractions 1 and 2 of gradients (c–e) are too high to be included.

the C protein in the medium pellet is a measure of the C protein in virus particles. The results are shown in Figure 10. In the case of the wt, most C (~80% of total) is found in the soluble NC pool immediately after the pulse. This decreases during the 5 h chase to ~65%. At the same time, an almost corresponding amount (~10%) of C protein is released as particles. These results are similar to those reported before for Sindbis virus formation (Scheele and Pfefferkorn, 1969). As the total amount of C protein in the sample remains somewhat constant (data not shown) this relationship suggests that intracellular NCs are precursors for the virions. However, there is also a significant fraction of non-extractable C protein present at all chase times. As so little of total C protein is used for virus formation, it cannot be excluded that this non-extractable C protein also plays a role in virus formation. In the case of the mutants the soluble C protein complexes, i.e. the NC intermediates and the ribosome-associated C protein, constitute 60–65% of all C protein after the pulse. During the chase this decreases to 30–35%. Only a small amount of this decrease can be accounted for by the released virus. This contains only ~5% of total C protein after the 5 h chase. The majority of the C protein (>60%) is found in the non-extractable fraction after the chase. Thus, while these results are also consistent with the soluble C protein complexes being precursors for virus, they do not exclude the possibility that the non-extractable pool is also involved.

The virus morphogenesis at cell surface was visualized directly using electron microscopy (Figure 9C–F). In the case of wt infected cells, pre-formed NCs can be seen at the cell surface in various stages of budding (Figure 9C and D). However, in the case of the mutants no preformed NCs were observed (Figure 9E and F). Rather, virus maturation appeared to follow a pathway where the NC matured concomitantly with virus budding (see budding profiles with underlying dense material). Eventually, particles with wt-like morphology were released from the cells.

Discussion

The most striking phenotype of the junction sequence deletion mutants was the total absence of cytoplasmic NCs.

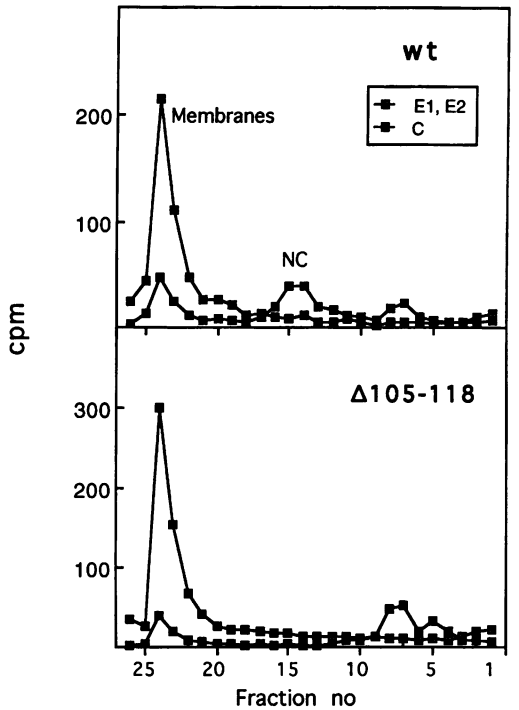

Fig. 8. Capsid and spike protein profiles of sedimented homogenates of transfected cells. Wild-type (wt) and SFV-CΔ105–118 RNA-transfected cells were pulse-labelled for 30 min with [^{35}S]methionine and chased for 30 min. Cell homogenates were prepared and samples of these were analysed by sedimentation on a 15–30% (w/w) sucrose gradient layered on a 1 ml 55% (w/w) sucrose cushion. Each fraction was analysed by SDS–PAGE for viral membrane (E1 and E2) and C proteins. The radioactivity content of the membrane and C proteins were quantified; amounts found in each fraction are shown. The top of each gradient is to the right.

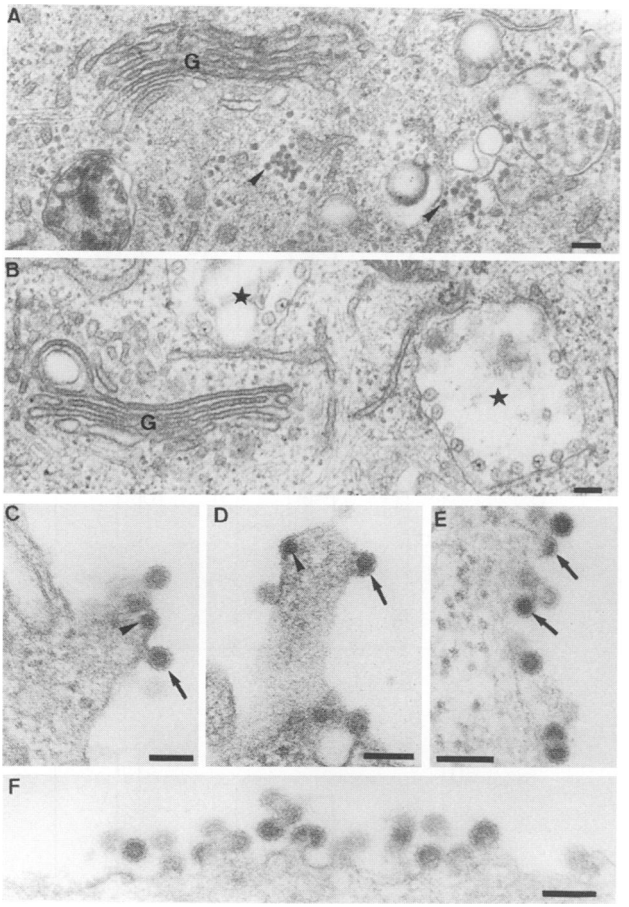

Fig. 9. Electron microscopic analyses of infected cells. Cytoplasm of (**A**) wt SFV-infected cells and (**B**) SFV-CΔ105–118 infected cells. Budding profiles of wt SFV are shown in (**C**) and (**D**) and those of SFV-CΔ105–118 in (**E**) and (**F**). Arrowheads, NCs; arrows, budding particles; G, Golgi complexes. Asterisks indicate cytoplasmic vacuoles of type I, which are typical for the infected cell. Bars represent 100 nm.

This was very surprising, especially when considering that wt-like particles were released from the infected or transfected cells with efficiencies which were rather similar to that of wt. The virtual absence of NCs was verified both biochemically by sedimentation analyses of NP-40 lysates and homogenates of transfected cells, and morphologically by EM analyses of sections of infected cells. Taken together, these results suggest that the conserved junction sequence is important for the assembly of a NC particle.

Recent cryo-electron microscopy and image processing analyses of RR and SFV NCs have revealed that the carboxy-terminal protease domain forms distinct pentameric and hexameric capsomers around the 5- and 2-fold axes of the NC particle (Cheng *et al.*, 1995; Fuller *et al.*, 1995). The interactions between individual protease domain monomers in the capsomers have been revealed with the help of the structure of the protease domain which has been determined by X-ray crystallographic analyses (Choi *et al.*, 1991) and which has been fitted into the EM structure of the whole particle. However, the exact positioning of the conserved junction sequence and the RNA-binding part of the C chain remain unidentified. It is possible that the conserved junction sequence represents an important element in stabilizing the capsomer–capsomer interactions.

Our analyses of the phenotypes of the mutants showed also that their infectivities were significantly reduced. The possible reason for this has not been investigated in this work; however, it has been suggested previously that the junction sequence that we have deleted acts as a signal for ribosome binding and genome uncoating during virus entry (Wengler *et al.*, 1992). In a recent report, Owen and Kuhn (1996) described a SIN C protein mutant with a deletion of residues 97–106, i.e. the proximal part of the conserved junction peptide. This mutant directed wt-like NC assembly in cytoplasm and also efficient particle release, but it encapsidated mostly viral 26S RNA instead of 42S RNA. A possible interpretation of these and our present results is that the proximal half of the junction sequence in alphaviruses serves in RNA encapsidation and the distal one in the stabilization of the NC. This model can be tested in future by analysing the RNA molecules (26S and 42S) of our SFV mutants. Still another possibility is that the reduced infectivity of our mutant particles is related to our finding of the tendency of their NCs to aggregate when the surrounding membrane is solubilized with NP-40. A corresponding aggregation could also take place after NC penetration into cytoplasm, during mutant virus entry and lead to non-productive infection.

It has been almost a dogma that alphaviruses use preassembled cytoplasmic NCs for virus budding. Our present results show that efficient particle formation can

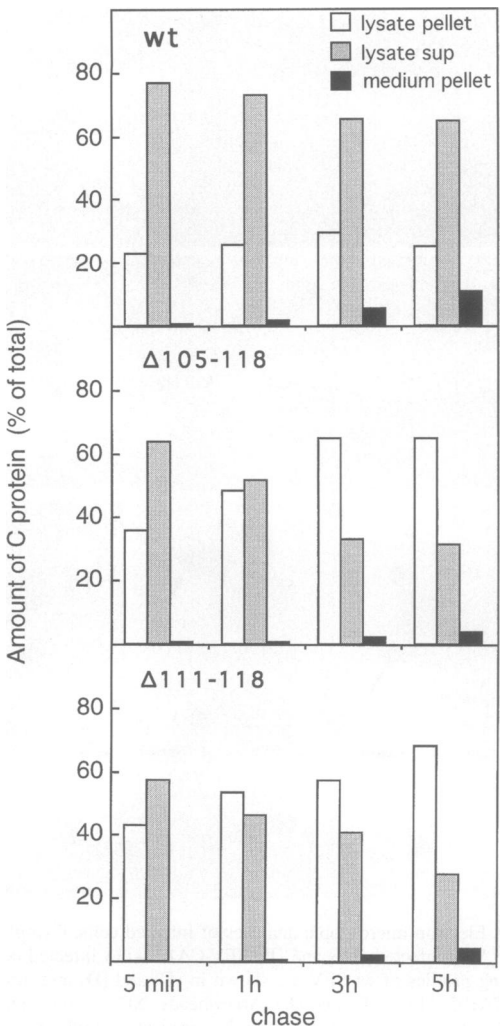

Fig. 10. Intracellular capsid complexes and virus release. Cells were transfected with wt or mutant RNA, pulse-labelled with [^{35}S]methionine for 15 min and chased as indicated. Cells were lysed in a NP-40-containing buffer and fractionated into a low-speed pellet and supernatant. The virus in media was pelleted. Samples of supernatants and pellets from lysates, and pellets from media, were subjected to analysis by SDS–PAGE and radioactive C protein was quantified. The columns show amount of C protein in each fraction as percentage of total C in the cell/media sample.

take place also without a cytoplasmic pool of NCs. How can this then be possible? We believe that the NC intermediate structures and the ribosome-associated C protein participate in an encapsidation process at the PM concomitantly with virus budding. We suggest that it is the interactions of the C proteins with the cytoplasmic parts of the transmembrane spikes at the PM which rescue the mutant C protein in their encapsidation process. This model is supported by our finding that the NCs of mutant viruses are apparently unstable and aggregate if the surrounding membrane is solubilized with NP-40. Furthermore, the model is consistent with the temporal relationship we found between the intracellular and the released viral C protein pools in our pulse–chase experiment, as well as with the budding profiles observed by EM analyses on the PM of mutant virus-infected cells. The means by which the spikes might mediate support for the NC assembly in the case of our mutants is probably not only a result of the membrane-anchoring of the NC complexes. According to the cryo-EM data of SFV and RR virus, the three heterodimers of each spike in the membrane bind to three C-monomers which are part of three different capsomers in the NC (Cheng *et al.*, 1995; Fuller *et al.*, 1995). This means that the spikes will cross-link the capsomers laterally together and thereby strengthen the NC. The lateral cross-linking effect of the spikes becomes even more evident when one considers the extensive spike–spike interactions on the external particle surface that are also revealed by the cryo-EM studies. These spike-mediated, lateral cross-linking effects are probably not only of importance for the maturation of the deletion mutants described here, but also for that of wt. Similar spike-mediated effects on virus maturation have been described for hepatitis B, vesicular stomatitis and coronaviruses (Simon *et al.*, 1988; Mebatsion *et al.*, 1996; Vennema *et al.*, 1996).

Recently, Skoging and co-workers described an SFV spike-gene deletion variant with a mutation in the remaining C gene, changing the codon for Tyr184 of the C protein to alanine, which had lost the capacity to express wt-like NCs in cell cytoplasm (Skoging *et al.*, 1996). Nevertheless, when cells expressing this mutant were co-transfected with a complementary C gene deletion variant that expressed SFV spikes, a small amount of infectious virus was released. It is possible also that in this case it is the binding of C proteins and/or incomplete NCs to the spikes that rescues the NC assembly process so that infectious viruses can be formed. It would be most interesting to introduce this mutation in a complete SFV genome and study virus morphogenesis at PM, intracellular capsid–RNA complexes and the relation of virus structure and function in more detail.

The assembly models that we describe above for the wt and the mutant SFV resemble in many respects those for the type D and C retroviruses, respectively (Wills and Craven, 1991; Hunter, 1994). According to the type D assembly model, which is used for instance by the Mason Pfizer Monkey virus (MPMV), the retrovirus capsids are assembled in cell cytoplasm and then transported to the cell surface for budding. Thus, although retrovirus budding is driven by direct capsid–membrane interactions, i.e. spikes are not needed for budding, the existence of a cytoplasmic pool of capsids, which are used for virus production, is very reminiscent of the wt alphavirus model. In contrast, in the type C model, which is representative for instance of the Moloney Murine Leukaemia virus, the capsid (the gag precursor) proteins encapsidate the genome concomitantly with budding at PM in a process which appears very similar to that observed by us for the SFV mutants. In the case of the type D retroviruses it is thought that their capsid subunits have strong enough intersubunit interactions to drive encapsidation in cytoplasm, whereas the type C virus have weaker ones and are therefore unable to do this. However, these weak interactions are sufficient to drive a complete encapsidation reaction when the gag precursors have been bound via their myristoylation modification to the PM. In this case it is understood that membrane binding of gag precursor molecules will, through the reduction of their dimensionality of movement, facilitate the formation of productive gag–gag interactions. The similarities between the assembly processes of the

retrovirus and those of the wt and mutant SFV are even more striking when one considers the surprising result with MPMV which showed that a single amino acid change in the gag precursor switched the D-type morphogenesis pathway of this virus into a C-type (Rhee and Hunter, 1990). Thus, this suggests that the basic assembly mechanism is probably very similar for both C- and D-type retroviruses and that a preassembled capsid in cytoplasm is not a prerequisite for productive budding in the case of the D-type viruses. Our present result with SFV suggests that this is apparently also not necessary for the alphaviruses.

Materials and methods

Materials

$Vent_R$ DNA polymerase was purchased from New England Biolabs (Beverly, USA). SP6 RNA polymerase, Cap [m7G (5′) ppp (5′) G] and protein A–Sepharose were from Pharmacia Biotech (Uppsala, Sweden). Media and reagents for cell culture were purchased from Gibco Laboratories Life Technologies Ltd (Paisley, UK). Actinomycin D was from Sigma Biochemicals (St Louis, MO). [^{35}S]Methionine (1000 Ci/mmol; SJ1515) was from Amersham International (Amersham, UK) and [^{3}H]uridine (1000 μCi/mmol; NET-367) from Du Pont-NEN Products (Boston, MA). SDS was from Bio-Rad (Cambridge, USA) and Nonidet P-40 (NP-40) from Fluka Chemie AG (Buchs, Switzerland). Sucrose was from J.T.Baker B (Deventer, Holland) and acrylamide/*bis*-acrylamide solution (29:1) from AT Biochem (Malvern, UK).

Cells and viruses

BHK-21 cells (American Type Culture Collection, Rockville, MD) were grown in BHK medium (Glasgow minimum essential medium) supplemented with 5% fetal calf serum (FCS), 10% tryptose phosphate broth, 2 mM glutamine and 20 mM HEPES. SFV was propagated in BHK-21 cells as previously described (Kääriäinen *et al.*, 1969; Wahlberg *et al.*, 1989).

Plasmid constructs

Plasmid pSFV-CΔ105–118. This contains a deletion in the C gene encompassing codons 105–118. To construct this we used plasmid pSP6–SFV4 (Liljeström and Garoff, 1991). First, we synthesized *in vitro* a 131 bp *Stu*I–*Csp*45I C gene fragment in which the C gene sequence from nucleotide 364 to nucleotide 406 had been deleted (numbering is from beginning of SFV 26 mRNA sequence; Garoff *et al.*, 1982). This was used to replace the wt 172 bp *Stu*I–*Csp*45I fragment of the C gene in pSP6–SFV4. The deleted fragment was synthesized by PCR using $Vent_R$ DNA polymerase. The primers used were: 5′-CCCAGCAGATGCAGCAAC-3′ (the 5′ end primer) and 5′- TAGCGCGTAATATTCGAAGATACA*TTTCTTCTTCTTCTTGTCGGC-3′ (the 3′ end primer). The 3′ end primer contains the deletion (*). Conditions for PCR were as recommended by the manufacturer.

Plasmid pSFV-CΔ111–118. This contains a deletion in the C gene encompassing codons 382–406. We first synthesized *in vitro* a 149 bp *Stu*I–*Csp*45I C gene fragment in which the C gene sequence from nucleotide 382 to nucleotide 406 had been deleted. This was used to replace the wt 172 bp *Stu*I–*Csp*45I fragment of the C gene in pSP6–SFV4. The primers used were: 5′-CCCAGCAGATGCAGCAAC-3′ (the 5′ end primer) and 5′- TAGCGCGTAATATTCGAAGATACA*TCTTTCTCTTTTTCCGGT-3′ (the 3′ end primer). The 3′ end primer contains the deletion (*).

In vitro transcription and RNA transfection

RNA transcripts were synthesized *in vitro* from *Spe*I-linearized plasmids (Liljeström and Garoff, 1991). RNA was transfected into BHK-21 cells by electroporation essentially as described by Suomalainen and Garoff (1994). In brief, 8×10^6 cells were suspended in 0.8 ml of Ca^{2+}/Mg^{2+}-free phosphate-buffered saline (PBS). The cell suspension was mixed with *in vitro*-made RNA (20 μl of the transcription mix), transferred to a 0.4 cm electroporation cuvette and exposed to two consecutive pulses at 0.85 kV and 25 μF using a Bio-Rad Gene Pulser (without the pulse controller unit). Electroporated cells were diluted in 18 ml BHK medium, plated in 35 mm tissue culture dishes and incubated at 37°C.

Virus isolation, plaque titration and infection

Stocks of SFV-CΔ105–118 and SFV-CΔ111–118 were prepared using cells that had been transfected with the corresponding RNA, essentially as described earlier for wt virus and stored in small aliquots at –70°C (Wahlberg *et al.*, 1989; Forsell *et al.*, 1995). BHK-21 cell monolayers were infected with wt or mutant virus at a m.o.i. of 10. After a 1 h absorption at 37°C, the medium was replaced with fresh Eagle's minimal essential medium (EMEM) and cells were further incubated. The infectivity of virus particles produced from infected or transfected cells was determined by conventional plaque assay on BHK-21 cell monolayers as described previously (Wahlberg and Garoff, 1992). Particles labelled with ^{35}S or double-labelled with ^{3}H and ^{35}S were isolated from media by centrifugation. The media sample was layered on top of a two-step sucrose gradient [1.0 ml 55% (w/w) and 5 ml 10% (w/w) sucrose in 50 mM Tris–HCl pH 7.4, 100 mM NaCl and 0.5 mM EDTA (TNE)]. Gradients were run at 30 000 r.p.m. for 90 min at 4°C in an SW40 rotor. Fractions were collected from below and the position of radioactive virus identified by liquid scintillation counting.

Metabolic labelling of cells with radioactive precursors

Labelling with [^{35}S]methionine. At 7 h after transfection cells were first starved for 30 min in methionine-free EMEM supplemented with 20 mM HEPES. The medium was replaced with the same medium containing 100 μCi/ml of [^{35}S]methionine and cells were incubated for 15 or 30 min at 37°C. After the pulse, cells were washed once with EMEM containing 20 mM HEPES and a 10-fold excess of non-radioactive methionine and incubated in the same medium for various times. Alternatively, cells were continuously labelled for 6 h with [^{35}S]methionine (100 μCi/ml).

Double-labelling with [^{3}H]uridine and [^{35}S]methionine. This was done using infected cells in 60 mm dishes, with actinomycin D (1 μg/ml) present in all incubation media. [^{3}H]Uridine labelling was started at 2.5 h post-infection (p.i.) by the addition of 25 μCi of isotope and continued until 10 h p.i. [^{35}S]Methionine labelling was started at 4 h p.i. by addition of 10 μCi (virus particle isolation) or 100 μCi (analysis of intracellular NCs) of isotope and continued also until 10 h p.i. During the time of [^{35}S]methionine labelling, a methionine-free medium was used.

Preparation of cell lysate, cell homogenate and virus pellets

Cells were put on ice, washed twice with ice-cold PBS and lysed in 300 μl lysis buffer (50 mM Tris–HCl pH 7.5, 1% NP-40, 10 mM iodoacetamide, 2.5 mM PMSF, 2 μg aprotinin/ml, 5 μg antipain/ml, 0.5 μg leupeptin/ml, 0.7 μg pepstatin/ml). The lysates were collected in Eppendorf tubes and non-extracted material was pelleted by low-speed centrifugation (6000 r.p.m. for 5 min at 4°C). The supernatants and pellets were analysed separately.

For homogenization, cells were collected by scraping in an ice-cold homogenization buffer [10 mM Tris–HCl pH 7.4, 1 mM EDTA, 2.5 mM PMSF/ml, 10% (w/w) sucrose] (Chong and Rose, 1993). Cells were disrupted by 20 strokes in a 23-gauge needle. A post-nuclear supernatant was prepared by centrifugation of the mixture at low speed as described above.

The culture media with virus were subjected to low-speed centrifugation to remove cell debris and thereafter virus particles were purified by pelletization through a 100 μl 10% (w/w) sucrose cushion (in TNE) in an Eppendorf tube using a Beckman JA 18.1 rotor at 17 000 r.p.m. for 2 h at 4°C. The pellets were resuspended in gel-sample buffer (Wahlberg *et al.*, 1989). The corresponding supernatants as well as the unfractionated cleared media were subjected to TCA precipitation. This was done by adding 100 μl of 20% TCA to the same volume of media. Precipitates were taken up into gel-sample buffer.

NP-40 treatment of virus

Membranes of purified virus particles were solubilized by incubation for 10 min at 0°C in 150 μl TNE which had been diluted 1:1 with water and which contained 1% NP-40.

Sedimentation analyses

Samples of virus, NP-40 treated virus, lysates or homogenates (150 μl) were analysed by sedimentation in 15–30% (w/w) sucrose gradients (12 ml) in TNE buffer. For analysis of NP-40-treated virus the gradient contained 0.1% NP-40 and, in the case of cell lysate analyses, in addition either $MgCl_2$ (1.5 mM) or EDTA (1 mM). For analysis of a cell homogenate the gradient contained EDTA (1 mM). In the latter case the 15–30% gradient was supplemented with a 1 ml 55% (w/w) sucrose

cushion (in TNE) at bottom. Before analysing lysates or homogenates in the EDTA-containing gradient the samples were incubated with EDTA (25 mM) for 30 min at 0°C to dissociate polysomes. The sedimentations were done in a SW41 rotor at 40 000 r.p.m. for 1.5 h (virus particles) or 2 h (cell lysate- and NP-40 treated virus samples) at 4°C. Gradients were fractionated from the bottom and aliquots taken up directly in gel-sample buffer or mixed with scintillation liquid.

Scintillation counting

Samples (100 μl) were mixed with scintillation liquid (3 ml) (Emulsifier-Safe) and radioactivity was counted in a 1410 Wallac scintillation counter using a standard program for ^{35}S or $^{35}S/^{3}H$ double-label.

SDS–PAGE

Electrophoresis was done in gels with 10% acrylamide as described previously (Wahlberg *et al.*, 1989). These were processed for autoradiography (Suomalainen *et al.*, 1990). The radioactivity in protein bands was determined by using a Bas-III Image Plate and the Fujix Bio-Image analyser system Bas 2000 (Fuji Photo Film Co.).

Electron microscopy

At ~6 h p.i., cells were incubated with fixation solution (2% glutaraldehyde, 0.1 M sodium cacodylate buffer pH 7.4) for 20 h at 37°C. Cells were scraped off and collected by pelletization. Following a wash in 0.1 M sodium cacodylate buffer, the cells were incubated in post-fixation solution (2% osmium tetroxide, 0.1 M sodium cacodylate pH 7.4) for 2 h at 4°C. The samples were then dehydrated for 15 min in first 70%, then 95%, and finally 100% ethanol at 4°C. Uranyl acetate (2%) was added to the final dehydration step. Following this, cells were placed in pure acetone for 15 min and embedded in LX-112 epon resin (Ladd, VT) and polymerized at 60°C. Ultra-thin sections were contrasted with uranyl acetate and lead citrate and analysed in a Philips 420 electron microscope at 80 kV.

Acknowledgements

The authors would like to thank Dr Mathilda Sjöberg for help with the 1410 Wallac scintillation counter, Dr Kjell Hultenby for EM analysis, Leena Rinnevuo for cell culture, Ingrid Sigurdson for typing and Dr Dirk-Jan Opstelten for critical reading of the manuscript. This work was supported by EU grants CHRX-CT94-496 and CHRX-CT92-0018, and the Swedish Natural Science Research Council (B-BU 09353-310).

References

Chang,G.-J.J. and Trent,D.W. (1987) Nucleotide sequence of the genome region encoding the 26S mRNA of Eastern equine encephalitis virus and the deduced amino acid sequence of the viral structural proteins. *J. Gen. Virol.*, **68**, 2129–2142.

Cheng,H.R., Kuhn,R.J., Olson,N.H., Rossmann,M.G., Choi,H.-K., Smith,T.J. and Baker,T.S. (1995) Nucleocapsid and glycoprotein organization in an enveloped virus. *Cell*, **80**, 621–630.

Choi,H.-K., Tong,L., Minor,W., Dumas,P., Boege,U., Rossmann,M.G. and Wengler,G. (1991) Structure of Sindbis virus core protein reveals a chymotrypsin-like serine proteinase and the organization of the virion. *Nature*, **354**, 37–43.

Chong,L.D. and Rose,J.K. (1993) Membrane association of functional vesicular stomatitis virus matrix protein *in vivo*. *J. Virol.*, **67**, 407–414.

Dalgarno,L., Rice,C.M. and Strauss,J.H. (1983) Ross River virus 26S RNA: complete nucleotide sequence and deduced sequence of the encoded structural proteins. *Virology*, **129**, 170–187.

Forsell,K., Suomalainen,M. and Garoff,H. (1995) Structure/function relation of the NH_2-terminal domain of the Semliki Forest virus capsid protein. *J. Virol.*, **69**, 1556–1563.

Fuller,S.D., Berriman,J.A., Butcher,S.J. and Gowen,B.E. (1995) Low pH induces swiveling of the glycoprotein heterodimers in the Semliki Forest virus spike complex. *Cell*, **81**, 715–725.

Garoff,H., Frischauf,A.M., Simons,K., Lehrach,H. and Delius,H. (1980) The capsid protein of Semliki Forest virus has clusters of basic amino acids and prolines in its amino-terminal region. *Proc. Natl Acad. Sci. USA*, **77**, 6376–6380.

Garoff,H., Kondor-Koch,C. and Riedel,H. (1982) Structure and assembly of alpha viruses. A review. *Curr. Top. Microbiol. Immunol.*, **99**, 1–50.

Geigenmüller-Gnirke,U., Nitschko,H. and Schlesinger,S. (1993) Deletion analysis of the capsid protein of Sindbis virus: identification of the RNA binding region. *J. Virol.*, **67**, 1620–1626.

Hahn,C.S., Lustig,S., Strauss,E.G. and Strauss,J.H. (1988) Western Equine encephalitis virus is a recombinant virus. *Proc. Natl Acad. Sci. USA*, **85**, 5997–6001.

Hunter,E. (1994) Macromolecular interactions in the assembly of HIV and other retroviruses. *Semin. Virol.*, **5**, 71–83.

Kinney,R.M., Johnson,R.J.B., Brown,V.L. and Trent,D.W. (1986) Nucleotide sequence of the 26S mRNA of the virulent Trinidad donkey strain of Venezuelan equine encephalitis virus and deduced sequence of the encoded structural proteins. *Virology*, **152**, 400–413.

Kääriäinen,L. and Söderlund,H. (1971) Properties of Semliki Forest virus nucleocapsid. I. Sensitivity to pancreatic ribonuclease. *Virology*, **43**, 291–299.

Kääriäinen,L., Simons,K. and von Bonsdorff,C.-H. (1969) Studies in subviral components of Semliki Forest virus. *Ann. Med. Exp. Fenn.*, **47**, 235–248.

Laine,R., Söderlund,H. and Renkonen,O. (1973) The chemical composition of Semliki Forest virus. *Intervirology*, **1**, 110–118.

Levinson,R., Strauss,J.H. and Strauss,E.G. (1990) Determination of the complete nucleotide sequence of the genomic RNA of O'Nyong-nyong virus and its use in the construction of phylogenetic trees. *Virology*, **175**, 110–123.

Liljeström,P. and Garoff,H. (1991) A new generation of animal cell expression vectors based on the Semliki Forest virus replicon. *BioTechnology*, **9**, 1356–1361.

Liljeström,P., Lusa,S., Huylebroeck,D. and Garoff,H. (1991) In vitro mutagenesis of a full-length cDNA clone of Semliki Forest virus: the 6,000-molecular-weight membrane protein modulates virus release. *J. Virol.*, **65**, 4107–4113.

Mebatsion,T., König,M. and Conzelmann,K.-K. (1996) Budding of rabies virus particles in the absence of the spike glycoprotein. *Cell*, **84**, 941–951.

Owen,K. and Kuhn,R.J. (1996) Identification of a region in the Sindbis virus nucleocapsid protein that is involved in specificity of RNA encapsidation. *J. Virol.*, **70**, 2757–2763.

Paredes,A.M., Brown,D.T., Rothnagel,R., Chiu,W., Schoepp,R.J., Johnston,R.E. and Prasad,B.V.V. (1993) Three-dimensional structure of a membrane-containing virus. *Proc. Natl Acad. Sci. USA*, **90**, 9095–9099.

Rhee,S.S. and Hunter,E. (1990) A single amino acid substitution within the matrix protein of a type D retrovirus converts its morphogenesis to that of a type C retrovirus. *Cell*, **63**, 77–86.

Rice,C.M. and Strauss,J.H. (1981) Nucleotide sequence of the 26S mRNA of Sindbis virus and deduced sequence of the encoded virus structural proteins. *Proc. Natl Acad. Sci. USA*, **78**, 2062–2066.

Rümenapf,T., Strauss,E. and Strauss,J. (1995) Aura virus is a new world representative of Sindbis-like viruses. *Virology*, **208**, 621–633.

Scheele,C.M. and Pfefferkorn,E.R. (1969) Kinetics of incorporation of structural proteins in Sindbis virions. *J. Virol.*, **3**, 369–375.

Simon,K., Lingappa,V.R. and Ganem,D. (1988) Secreted hepatitis B surface antigen poly-peptides are derived from a transmembrane precursor. *J. Cell Biol.*, **107**, 2163–2168.

Skoging,U., Vihinen,M., Nilsson,L. and Liljeström,P. (1996) Aromatic interactions define the binding of the alphavirus spike to its nucleocapsids. *Structure*, **4**, 519–529.

Söderlund,H. (1973) Kinetics of formation of the Semliki Forest virus nucleocapsid. *Intervirology*, **1**, 354–361.

Söderlund,H. and Ulmanen,I. (1977) Transient association of Semliki Forest virus capsid protein with ribosomes. *J. Virol.*, **24**, 907–909.

Strauss,J.H. and Strauss,E.G. (1994) The alphaviruses: gene expression, replication and evolution. *Microbiol. Rev.*, **58**, 491–562.

Suomalainen,M. and Garoff,H. (1994) Incorporation of homologous and heterologous proteins into the envelope of Moloney murine leukemia virus. *J. Virol.*, **68**, 4879–4889.

Suomalainen,M., Baron,M. and Garoff,H. (1990) The E2 signal sequence of Rubella virus remains part of the capsid protein and confers membrane association *in vitro*. *J. Virol.*, **64**, 5500–5509.

Suomalainen,M., Liljeström,P. and Garoff,H. (1992) Spike protein-nucleocapsid interactions drive the budding of alphaviruses. *J. Virol.*, **66**, 4737–4747.

Ulmanen,I. (1978) Assembly of Semliki Forest virus nucleocapsid: detection of a precursor in infected cells. *J. Gen. Virol.*, **41**, 353–365.

Ulmanen,I., Söderlund,H. and Kaariainen,L. (1976) Semliki Forest virus capsid protein associates with the 60S ribosomal subunit in infected cells. *J. Virol.*, **20**, 203–210.

Vennema,H., Godeke,G.-J., Rossen,J.W.A., Voorhout,W.F., Horzinek,M.C., Opstelten,D.-J.E. and Rottier,P.J.M. (1996) Nucleo-

capsid-independent assembly of coronavirus-like particles by co-expression of viral envelope protein genes. *EMBO J.*, **15**, 2020–2028.
Vogel,R.H., Provencher,S.W., von Bonsdorff,C.-H., Adrian,M. and Dubochet,J. (1986) Envelope structure of Semliki Forest virus reconstructed from cryo-electron micrographs. *Nature*, **320**, 533–535.
Wahlberg,J. and Garoff,H. (1992) Membrane fusion process of Semliki Forest virus I: low pH-induced rearrangement in spike protein quaternary structure precedes virus penetration into cells. *J. Cell Biol.*, **116**, 339–348.
Wahlberg,J.M., Boere,W.A. and Garoff,H. (1989) The heterodimeric association between the membrane proteins of Semliki Forest virus changes its sensitivity to mildly acidic pH during virus maturation. *J. Virol.*, **63**, 4991–4997.
Weiss,B., Nitschko,H., Ghattas,I., Wright,R. and Schlesinger,S. (1989) Evidence for specificity in the encapsidation of Sindbis virus RNAs. *J. Virol.*, **63**, 5310–5318.
Wengler,G., Würkner,D. and Wengler,G. (1992) Identification of a sequence element in the alphavirus core protein which mediates interaction of cores with ribosomes and the disassembly of cores. *Virology*, **191**, 880–888.
Wills,J.W. and Craven,R.C. (1991) Form, function, and use of retroviral Gag proteins. *AIDS*, **5**, 639–654.

Received on July 9, 1996; revised on August 28, 1996